

BENCHMARKING OF TRANSIENT CODES AGAINST CYCLE 19 STABILITY MEASUREMENTS AT LEIBSTADT NUCLEAR POWER PLANT (KKL)

**Carlos Aguirre^{a*}, Stefan Opel^b, Hakim Ferroukhi^c, Gerardo Grandi^d,
Lotfi Belblidia^e, Mats Thunman^f, Camilla Rotander^f, Bengt-Göran Bergdahl^g,
Simon Baumgartner^h, Guido Ledergerber^a**

^a Kernkraftwerk Leibstadt AG, Leibstadt, Aargau, Switzerland

^b AREVA NP GmbH, Erlangen, Bayern, Germany

^c Paul Scherrer Institut, Villigen, Aargau, Switzerland

^d Studsvik Scandpower Inc., Idaho Falls, Idaho, USA

^e Studsvik Scandpower Inc., Gaithersburg, Maryland, USA

^f Westinghouse Electric Sweden AB, Västerås, Västmanland, Sweden

^g GSE Power Systems AB, Nyköping, Södermanland, Sweden

^h AXPO AG, Baden, Aargau, Switzerland

*** Corresponding author**

carlos.aguirre@kkk.ch

Tel: + 41 56 267 8353, fax number: + 41 56 267 7790

ABSTRACT

Coupled neutronics-thermal hydraulic codes are used by many utilities, research institutes and regulatory authorities worldwide for performing BWR stability analysis. RAMONA-3 has been established in the industry for quite a long time as a reliable time-domain dynamic code with best performance for predictive calculations. Next generation of codes such as RAMONA-5, SIMULATE-3K and POLCA-T, with advanced two-group neutronics and more detailed plant description and thermal hydraulics models have been introduced. The performance of these codes against the stability measurements performed in cycle 19 at the Swiss nuclear power plant Leibstadt (KKL), a BWR/6 from General Electric, is presented in this paper. Important suppliers of the nuclear industry such as Westinghouse Electric Sweden, AREVA NP Germany, Studsvik Scandpower Inc. USA, and the Swiss research institute PSI have participated in this work. The validation of calculation methods against the KKL stability measurements was considered important by the various organizations for different reasons. Amongst others, Studsvik Scandpower aimed at filling a gap in the SIMULATE-3K stability benchmark database to include a jet pumps driven plant, AREVA NP had to fulfill fuel licensing requirements, and Westinghouse planned to launch POLCA-T parallel to a validation of RAMONA-5 as a production code. PSI cooperated with KKL in stability issues from the very beginning and introduced the stability test project in the framework of NACUSP, a European consortium that aimed for a better understanding of the BWR stability problem. For that purpose, this validation provides an assessment of advanced stability codes for modern BWR core designs.

Key Words: BWR Stability Oscillation Resonance Decay-ratio Transient-code

1. INTRODUCTION

An accurate determination of the stability parameters, i.e. decay ratio (DR) and resonance frequency (RF), is a primary feature of dynamic codes. For the completion of Leibstadt Nuclear Power Plant (KKL) power uprate, stability tests were performed in cycle 19 on September 1st 2002 [1]. In this context the opportunity arose to validate and benchmark different transient codes for stability analysis. The prediction of the stability behavior for a heterogeneous core loaded with a substantial amount of modern fuel bundles with partial length rods might impose novel demands to the entire reactor analysis computation route including at the end the applied coupled neutronics-thermal hydraulic code.

The organizations involved in this work together with the codes used for the simulations are listed below. Since RAMONA is used by different organizations but utilizing their own plant models, acronyms (e.g. AR3) are used to distinguish the different contributions.

AREVA NP GmbH	RAMONA-3 (AR3) [2]
Paul Scherrer Institut (PSI)	RAMONA-3 (PR3) [3]
Studsvik Scandpower Inc. (SSP)	RAMONA-5 (SR5) [4] and SIMULATE 3K (S3K) [5]
Westinghouse Electric Sweden AB (WSE)	RAMONA-5 (WR5) [6] and POLCA-T (P-T) [7]

The aim of this paper is to summarize and compare the stability results performed with different methodologies against the measured values obtained by noise analysis of the neutron detector signals (LPRM). PSI [8] and GSE Power Systems AB [9] have used different methodologies to determine the measured values.

2. STABILITY OF A BWR

The stability of a boiling water reactor (BWR) is of great importance for optimum plant performance. It has been observed that large BWRs in current operation could experience a less stable behavior under certain conditions with low coolant flow and unfavorable core power distributions. These conditions may prevail during startup or shutdown of the plant, during power maneuvers or as a result of runbacks or trip of reactor recirculation pumps.

Density wave oscillations constitute the basic phenomenon for coupled neutronics-thermal hydraulic instabilities [10]. Due to the strong influence of the coolant on the neutron population in the reactor, as it also serves as moderator, oscillations in the coolant flow rate and void fraction result in power oscillations in BWRs. The strength of the coupling between the thermal hydraulics and the neutronics, the void reactivity feedback, has an important effect on the stability of the BWR.

Examples of interaction between neutronics and thermal hydraulics leading to BWR oscillations have been observed in several operating plants. Typically two types of oscillations have been observed: in-phase (core wide) oscillations and out-of-phase (regional) oscillations. Regional oscillations tend to occur more often in large cores compared to smaller cores. During this sort of oscillations the power in one region of the core oscillates out of phase with respect to power of other regions. The inlet flows to the different regions are also out of phase with respect to each other. The averaged measured core power (APRM) keeps however constant, making this type of oscillations difficult to detect. On the contrary, in-phase oscillations, where the power and the flow oscillate simultaneously on the whole core, are easily detected through the APRM output. Out-of-phase oscillations are damped by the higher neutron harmonic mode (first azimuthal mode) whereas in-phase oscillations, which are thermo hydraulically more stable, are destabilized by the strong feedback from the fundamental neutronic mode [11].

Modern fuel assemblies with partial length rods have been lately introduced with the aim to improve shutdown margins and thermal limits and also the stability performance due to the decreased two-phase pressure drop. These increased margin improvements are normally used for optimization of the core design providing for a more bottom peaked axial power shape and more negative void reactivity coefficient, which in turn can have a negative impact on the stability. Despite the increased channel stability using partial length rods, the fuel development implies possibilities in reload optimization which could seemingly deteriorate the core stability.

The most accurate way to determine the core stability margin is through plant tests. On five occasions, stability tests have been performed at KKL. Of special interest are the tests performed at the beginning of cycle 7, 10 and 19. In cycle 10 [12] and cycle 19 [1] tests only in-phase oscillations were observed. In cycle 7 test out-of-phase oscillations were observed [12] but could not be confirmed in cycle 19.

3. CYCLE 19 STABILITY MEASUREMENTS

Cycle 19 stability measurements constituted the last commitment that KKL had to fulfill to conclude the plant power uprate licensing from 3138 to 3600 MW. The test was planned and carried out in collaboration with PSI in the framework of NACUSP project [13].

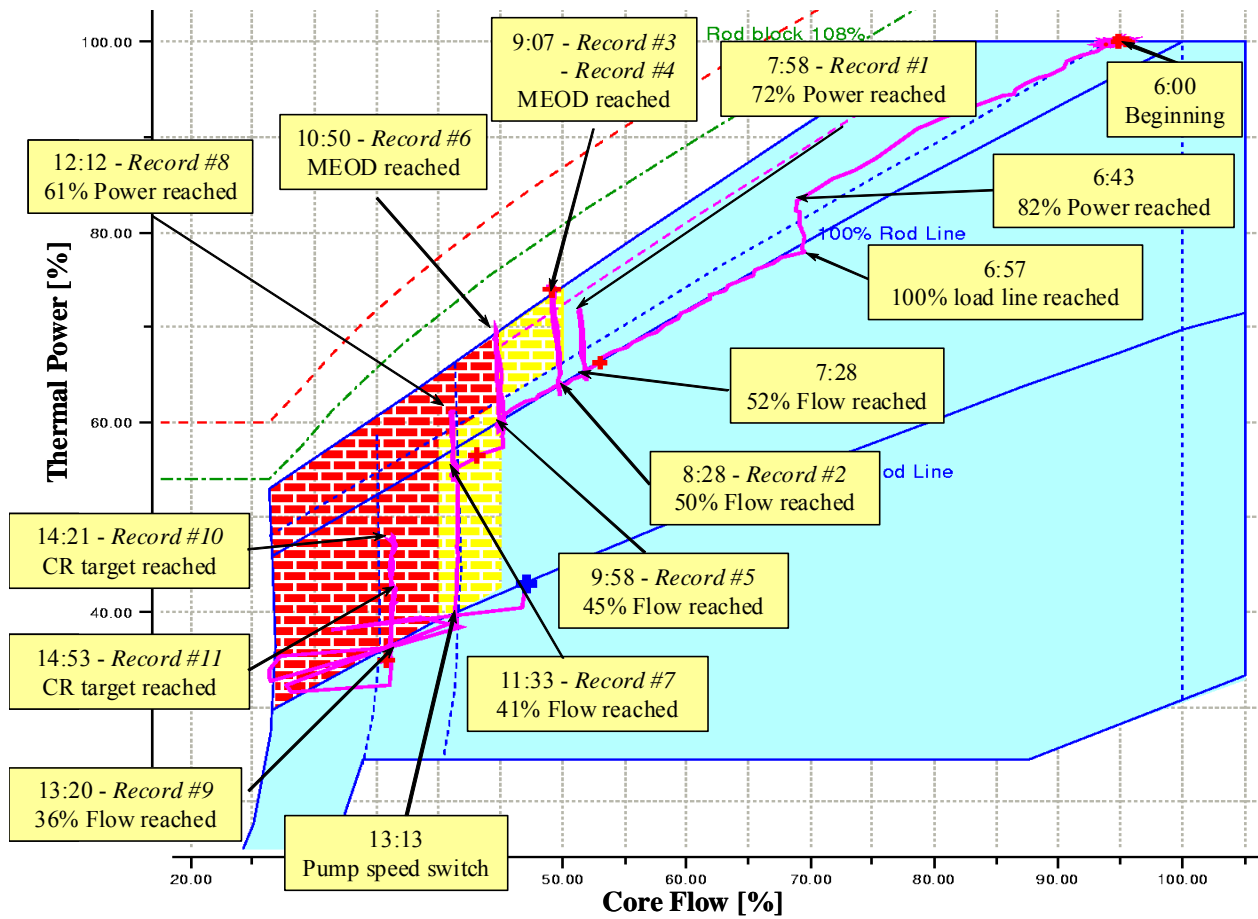


Figure 1: Course of cycle 19 stability test

The operating points were selected based on the background provided by earlier tests and modern objectives in conjunction with PSI and NACUSP. Primarily the measurements were performed to validate the current Maximum Extended Operating Domain (MEOD) line in the uprated power flow map as well as its analytically defined boundaries for stability monitoring and excluding regions. Other important goals were the verification of the dynamic characteristics of the core with an increasing inventory (>60%) of fuel assemblies with partial length rods and the qualification of the core stability monitoring system COSMOS, developed by ABB Atom, with regards to regional oscillations. COSMOS calculates online DR and oscillation frequency using noise analysis of 29 LPRM and 2 APRM signals with an 8 Hz sampling frequency.

A total of eleven test recordings were conducted (see Fig. 1), each lasting about 10 minutes, eight performed with the recirculation pumps running at high speed and three with the pumps in low speed mode. At constant flows the target powers were reached adjusting deep control rods. The recordings 3 and 4 have the same power and flow conditions but control rods in shallow positions were removed after recording 3 providing for a more bottom peaked axial power distribution from recording 4 upwards. Digital signal recordings of eight LPRM signals, all APRM signals (also 8), and a number of process signals (steam dome pressure, feedwater flow, steam flow, jet pump flow, reactor bottom drain line temperature, etc.) were made using the data acquisition system GETARS with a 40 Hz sampling frequency. These signals were later analyzed to extract DR and frequencies. At the same time, the DR and frequencies from COSMOS were recorded.

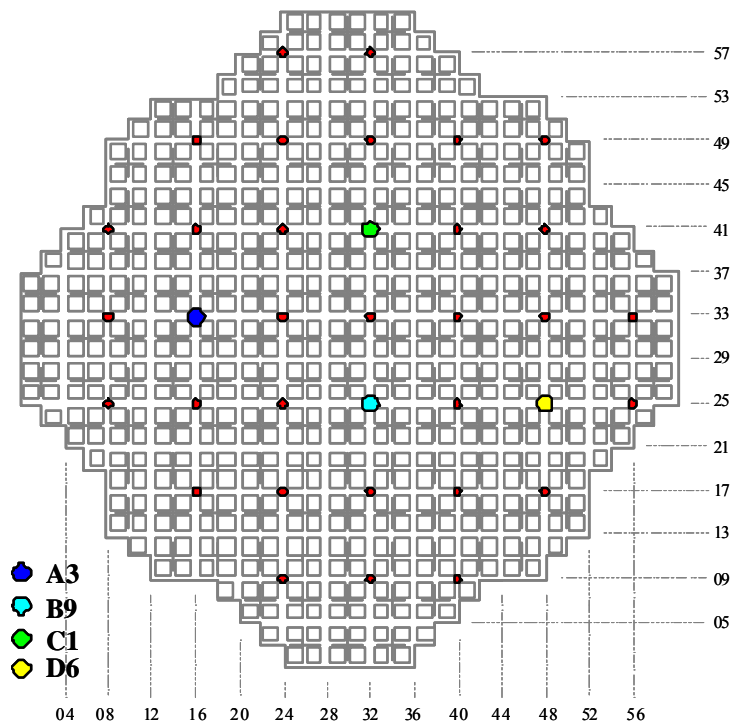


Figure 2: LPRM Strings selected for the TIP measurements

At each measurement point during the recording phase four simultaneous traversing in-core probe (TIP) campaigns were performed for LPRM strings belonging to different core quadrants and placed in

representative locations with regards to stability (see Fig.2). The data collected during the TIP campaigns have been used to verify the proper determination of core axial power distributions, which is of singular importance for the improvement of the modeling of the 3-D simulators.

Table I gives a summary of the principal operating parameters that prevailed during the stability measurements. Core thermal power and core inlet subcooling are based on online calculations of the heat balance module whereas core flow and steam dome pressure are plant measurements. The nominal values of core thermal power and total core flow at KKL are 3600 MW and 11151 kg/s respectively.

Table I: Summary of measured results in cycle 19

Case	Power (%)	Flow (%)	Subcooling (kJ/kg)	Pressure (bar)
1	72.16±0.09	51.34±0.08	88.67±0.15	69.84±0.01
2	62.93±0.10	49.87±0.07	83.00±0.15	69.00±0.01
3	74.44±0.07	49.11±0.10	94.91±0.20	70.06±0.01
4	73.94±0.08	49.14±0.10	94.35±0.15	70.02±0.01
5	59.33±0.09	44.82±0.08	88.93±0.18	68.72±0.01
6	69.99±0.06	44.61±0.10	100.43±0.22	69.65±0.01
7	53.93±0.08	41.26±0.04	90.62±0.16	68.33±0.01
8	61.08±0.06	41.03±0.04	99.56±0.13	68.86±0.01
9	34.94±0.10	35.93±0.10	76.82±0.28	67.27±0.01
10	47.58±0.06	36.33±0.06	96.11±0.18	67.93±0.01
11	42.58±0.08	36.31±0.09	88.43±0.25	67.65±0.01

4. REACTOR SIGNAL TIME SERIES ANALYSIS

PSI and GSE have used different methodologies to perform noise analysis of the neutron detector signals (APRM, LPRM) collected during the recordings of the cycle 19 stability tests. The resulting core stability parameters (i.e. DR and RF) are defined as the measured values valid for comparison to dynamic code results.

4.1 PSI Methodology

PSI has developed a systematic and consistent methodology to evaluate the BWR core stability parameters from measured reactor noise signal [8]. Basically, this methodology consists in a general reactor noise analysis where as much as possible information recorded during the tests is investigated prior to determining core representative stability parameters along with an associated estimate of the uncertainty range. A central part in this approach is that the evaluation of the core stability parameters is performed not only for a few but for all recorded neutron flux signals, allowing thereby the assessment of signal-related uncertainties. In addition, for each signal, three different model-order optimization methods are systematically employed to take into consideration the sensitivity upon the model order. The adopted methodology consists mainly of three phases: a screening phase, a neutron flux time series analysis and a core stability evaluation.

The first phase consists in the investigation of all recorded signals (i.e. not only the neutron flux signals but also all other process signals) with regards to signals variation, signal to noise ratios and spectral/cross spectral densities. The aim of this investigation is to detect possible trends and/or assess the eventual impact of external disturbances (e.g. process variations induced by control systems or non-stationary test conditions) on the core response. During the screening step cross-spectral and coherence analysis between all LPRM signals is performed in order to detect out-of-phase oscillations. In the second phase, a time series analysis (TSA) is performed for all measured neutron flux signals to determine the signal specific stability parameters (DR, RF). The TSA procedure consists in evaluating for each signal, the stability parameters using an auto regressive moving average (ARMA) modeling approach and applying systematically, three optimization methods for the model order selection: 1) Plateau Method, 2) Aikake Information Criterion (AIC) and 3) Rissanen Minimum Description Length (MDL). The application of these three optimization procedures, made through the HPTSAC code [14], yields three pairs of stability parameters for each neutron flux signal. For each type of signal (i.e. APRM, LPRM), average DR and RF values are estimated as function of the optimization method along with an associated standard deviation referred to as the method-averaged spread. Similarly, for each optimization method, average DR and RF values are estimated for all signals along with an associated standard deviation referred to as the signal-averaged spread. Thereafter, a core representative DR or RF is evaluated based on the APRM results averaged over all signals and methods. The LPRM-averaged spread and the APRM-averaged spread from the core representative DR or RF are as a last step computed and the maximum value of these two quantities is finally selected as the uncertainty range associated with the evaluated core representative stability parameter. A very detailed description of both the method-averaged spread and the signal-averaged spread can be found in reference [8].

4.2 GSE Methodology

GSE has more than 50 man-year experience of stability analysis and has developed its own methods of data reduction for BWR stability evaluation. GSE applies the so called process identification technique with a sliding data window. It is a signal processing technique to determine the process dynamics through fitting a mathematical model to a set of sampled data series. It allows the stability parameter evaluation as a function of time. The methodology has been embedded into the noise analysis program BRUS that contains several tools to perform stability evaluation. It basically consists of three phases: diagnostics check, signal pre-processing and core stability evaluation.

The diagnostics check is performed with dedicated signal evaluation programs to assay the quality and suitability of the data for the analysis of the stability evaluation. Signal recording conditions as data sampling frequency or reactor state during the recordings are checked. Next, undesirable behaviour in the recorded signal such as sensor failure, signal saturation, harmful noise, non-stationary of the data series, bit deficiency etc. are examined.

The signal pre-processing is carried out where harmful noise components have been removed using the pre-processing tools included in the BRUS package. Also, de-trending has to be made if necessary. At this stage the data sampling frequency is adjusted using the re-sampling program in BRUS so that all the data are analyzed under as similar condition as possible.

The stability evaluation is based on process identification techniques. An auto regressive (AR) model based on Levinsson algorithm is applied. A size of series data is assigned, called data window. The data in the data window is used for process identification to estimate the stability parameters. In order to determine their time dependency, the data window is shifted forward by a predetermined size each time when the process identification is performed. The AR model identified in each data window is used to

estimate the DR and RF. They are obtained by checking the worst pole in the AR polynomial. The mean and standard deviation are calculated to present the scatter of the parameter estimates. The core representative stability parameter is therefore evaluated averaging the results from all the APRM results. The amplitude is estimated using a simple recursive method for 2nd order adaptive high-pass filter called double exponential smoother. It allows calculating the variance of the data series. The square root of the variance yields the estimate of signal amplitude as a function of time.

In summary, GSE’s approach focuses on the estimation of stability parameters as a function of time, which is similar to an on-line stability monitor. This is because the stability state often changes dynamically even when the data series appear to be stationary. Finally, a cross power spectrum calculation for a given pair of LPRM signals is done to detect possible out-of-phase oscillations. The spatial phase is the maximum phase in the frequency interval of 0.1 Hz around the averaged spectral peak value of LPRM involved in the evaluation. To calculate the phase curve multivariate AR modeling technique is applied.

4.3 Results of the Reactor Signals Analysis

The results from both approaches are summarized in Table II. It appears that GSE’s results either agree well with PSI’s results within the uncertainty band or are somewhat conservative. Due to the more comprehensive uncertainty evaluation the values of the PSI analysis has been chosen by KKL as the official reference for comparison with code results.

Table II: Summary of measured results* in cycle 19

Case	APRM Time Series Analysis			
	(PSI)		(GSE)	
	DR	RF	DR	RF
1	0.43±0.07	0.68±0.02	0.42±0.02	0.66±0.01
3	0.46±0.07	0.67±0.02	0.52±0.02	0.69±0.01
4	0.55±0.06	0.70±0.01	0.64±0.01	0.70±0.00
5	0.49±0.07	0.65±0.02	0.48±0.02	0.65±0.01
6	0.68±0.09	0.66±0.02	0.66±0.03	0.66±0.00
7	0.59±0.06	0.63±0.02	0.67±0.01	0.63±0.00
8	0.71±0.04	0.63±0.01	0.77±0.01	0.63±0.00
9	0.40±0.11	0.47±0.02	0.44±0.04	0.48±0.01
10	0.64±0.05	0.59±0.01	0.73±0.01	0.59±0.00
11	0.54±0.10	0.54±0.02	0.59±0.03	0.54±0.00

Figure 3 depicts the official measured values of decay ratio in the operating map. At high powers within the stability monitoring (supervised[†], yellow zone) and excluding (exclusion[‡], red zone) regions

* Recording 2 is not included in the analysis. A failure in the data acquisition made it too short and therefore inappropriate.

† Operation permitted with higher surveillance

‡ Operation strictly forbidden.

(Recordings 4, 6, 8, and 10) high decay ratios were expected. Accordingly, with exception of recording 7, values of decay ratio larger than 0.55 were measured solely at those operating points.

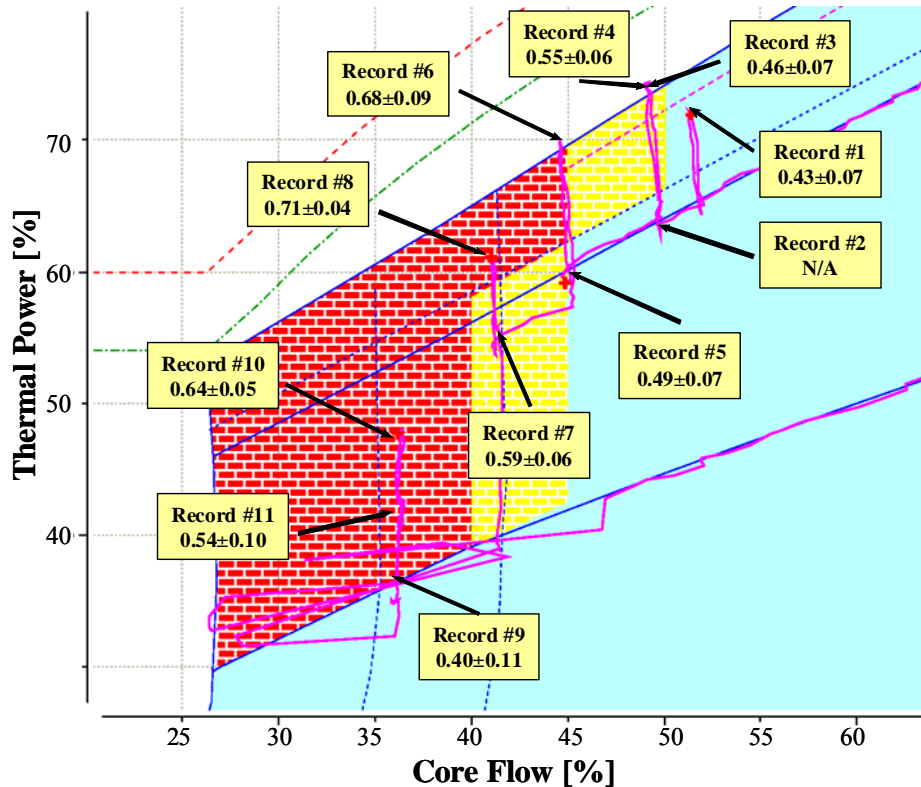


Figure 3: Result of the DR measurements in the Power Flow Map

5. STABILITY CALCULATIONS

The validation of calculation methods against the KKL cycle 19 stability measurements was considered important by the different organizations for various reasons. Amongst others, SSP aimed at filling a gap in the S3K stability benchmark database to include a jet pumps driven plant, AREVA NP (AR3) had to fulfill fuel licensing requirements, and WSE planned to launch POLCA-T (P-T) parallel to a validation of RAMONA-5 (WR5) as a production tool. PSI cooperated with KKL in stability issues from the very beginning [12] and introduced the stability test project in the framework of NACUSP [13].

Code validation is based on an extensive database of stability measurements for different reactor types, core loadings, fuel designs, operating conditions, oscillation modes etc. This database, which may differ somewhat for different codes, constitutes the validation for each code. The applied acceptance criteria are based, partly, on the code validation uncertainty. Each code differs in modeling and numerical methods, especially regarding modeling and correlations for slip, pressure drop and fuel thermodynamics. The uncertainty in input data might also differ due to level of detail in modeling. The KKL cycle 19 stability measurements constitutes only a subset of each code validation, and due to the possible differences above the code uncertainty for this subset might differ somewhat between the codes.

5.1 Codes Main Characteristics

RAMONA-3 (R3) is a detailed best-estimate thermal-hydraulic computer code with 3-D neutron kinetics. The neutronic model is based on a well established 1½-group diffusion theory, with all the fuel explicitly represented by 2-groups macroscopic cross section data in polynomial form. The thermal-hydraulics is based on a 4-equation model, vapor and liquid mass conservation, vapor and liquid energy conservation, with the mixture momentum equation integrated around the flow loop. Non-equilibrium phase velocities are accounted for a slip-correlation. Coolant subcooling and superheating are modeled. The time integration used a second order explicit scheme, whereas the neutronics is integrated with a predictor/corrector method in an implicit formulation.

RAMONA-5 (R5) includes both the 1½ group method from R3 and the advanced neutronic model based on 2-group diffusion theory. R5 has a detailed cross section representation based on tables which provides for a more accurate reactivity effects. The thermal-hydraulic model is the same as the one in R3.

S3K solves the 3-D, two-energy group, neutron diffusion equation. The core model uses a fourth-order flux expansion to represent the neutron flux shape within each node (in each of the three directions). Accuracy of the S3K core model depends not only on detailed 3-D neutronic and thermal-hydraulic modeling, but also on accurate representation of feedback parameters. Neutronic data is functionalized into a series of fuel type dependent 3-D table sets. The core is represented with one thermal-hydraulic channel per fuel bundle with no cross flow. The area-averaged form of the conservation equations employed in S3K is similar to that appearing in the literature. A six-equation model is used: vapor and liquid mass conservation, vapor and liquid energy conservation. Rather than solving the separate phasic momentum equations directly, it is convenient to use the mixture momentum equation and a weighted difference of the two phasic momentum equations. The general drift formulation for the void fraction completes the set of equations to be solved. The concentration parameter and the void-weighted drift velocity are calculated using the EPRI correlations. The subcooled boiling model is taken from Lahey's mechanistic model. A fuel pin model based on the INTERPIN code is built in S3K. All BWR vessel components except the steam dome and the bulk water regions (lump models) are modeled as 1-D components. S3K accounts for special models to represent the steam generator and the characteristics of the reactor recirculation pumps and the jet pumps.

POLCA-T incorporates a full 3-D neutronics model of the reactor core. Each fuel assembly in the core, including in- and inter-assembly bypass regions, may be represented in the thermal-hydraulic model. The reactor pressure vessel, external pump loops, steam system, feed-water system, emergency core cooling systems and steam relief system can be modeled to the desired details. The neutronics models in the code are the same as those in the steady state code POLCA7 with addition of proper kinetic terms for transient use. The thermal-hydraulic model includes thermal non-equilibrium between phases and has full geometric flexibility. The model solves the mass and energy conservation equations for each phase and for each volume cell. The momentum conservation equation is solved for each flow path. Constitutive equations are included for calculating the fluid properties and their derivatives. Empirical correlations are implemented for the calculation of pressure drops, fluid properties, solubility of non-condensable gases, phase flows (drift flux), and critical flow rate. The thermal model solves the heat conduction equation for the heat structures (fuel rods, pressure vessel, and internals) using heat transfer boundary conditions. The result is the heat transfer to the coolant. A complete range of convective heat transfer regimes is included in the code. The power generation models calculate the heat generation due to fission in the fuel, direct heat released in the coolant, and decay heat. A two group 3-D neutron kinetics model determines fission power. The 3-D-kinetics model is solved using an iterative method and is then iterated in an outer loop

including the thermal-hydraulic equations until convergence is reached. The hydraulic model can be solved using a fully implicit or semi-implicit method.

5.2 KKL Plant Calculation Model

The KKL models used in the different programs include similar features. The calculation model comprises the reactor pressure vessel with all important internal components (reactor core, upper plenum and riser, steam separator and dryer, steam dome, downcomer and lower plenum), steam lines and control systems. The jet pumps and recirculation loop are explicitly modeled. The behavior of the pumps is calculated based on specific jet pump data. The reactor core is described in full core geometry with 648 neutronic and hydraulic channels. That is one channel per bundle allocated in the core having each bundle type its specific hydraulic characteristics. The core bypass flow is modeled separately as one averaged channel. Twenty five axial nodes are used in each of the multiple core channels in order to obtain accurate axial power and void distributions. The recirculation loop, the downcomer, the lower and upper plenum, the steam separators with the risers and the steam dome are represented one-dimensionally by geometry, hydraulic parameters and pressure losses with segments divided up to several nodes.

5.3 Core Model Initialization

To initialize the models, different combinations of lattice physics and core design codes have been used by the various organizations to produce the cross sections, kinetic data, and neutronic history data (see Table III). Cross section data are parameterized with regards to fuel type, burnup, moderator density, density history, control rod presence, fuel temperature and Xenon concentration.

Table III: Cross Table Organization-Code used in the benchmarking

Organization	Acronym	Lattice Code	Steady State Code	Transient Code
AREVA NP	AR3	CASMO 4	MICROBURN-B2	RAMONA-3
PSI	PR3	CASMO 4	PRESTO-2	RAMONA-3
Studsvik Scandpower	SK3	CASMO 4	SIMULATE-3	S3K
Studsvik Scandpower	SR5	HELIOS	PRESTO-2	RAMONA-5
Westinghouse Nuclear Sweden	WR5	PHOENIX4	POLCA7	RAMONA-5 [§]
Westinghouse Nuclear Sweden	P-T	PHOENIX4	POLCA7	POLCA-T

AREVA NP, PSI and SSP use mainly CASMO-4 to produce the fuel type dependant cross sections and kinetic data for AR3, PR3 and S3K. WSE uses PHOENIX4 to generate such data for P-T and WR5. HELIOS has been used only for SSP SR5 calculations.

The initial conditions for the stability calculations at each measurement point have been obtained through steady state core calculations using stationary codes (MICROBURN-B2, SIMULATE-3, PRESTO-2, POLCA7). The performance of such codes at the off-rated conditions that prevailed during the test was

[§] Using 1½-group diffusion theory, similar to RAMONA-3

assessed on the basis of comparisons against TIP measurements performed during the recordings and with particular emphasis on the agreement in terms of the axial power profile, a key parameter affecting the core stability behavior. As an example Figure 4 shows the comparisons made against the TIP measurements in String B9 during the recording 8, the one which showed less stability. Double hump axial distributions as such in String B9 are challenging for the codes. S3K (actually SIMULATE-3) and MICROBURN-B2 showed better agreement than POLCA7 and PRESTO-2. Similar comparisons have been done for the rest of the selected operating points.

For each stability calculation, the reactor history in form of nodal distributions (e.g. exposure, void history, xenon) is passed from the steady state simulator to the transient code (see Table III). Historically PSI uses the CASMO-SIMULATE package for core analysis, but for this specific study PSI has used history data and flow distributions coming from PRESTO-2.

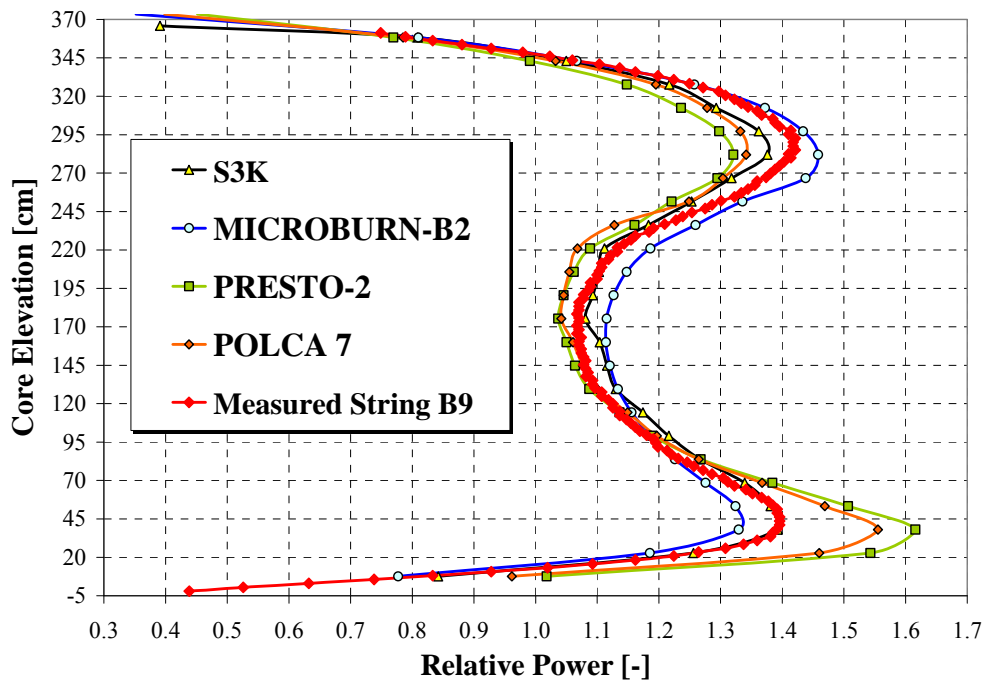


Figure 4: TIP Comparison Recording 8 String B9

5.4 Transient Analysis

The transient simulation is normally initiated by a control rod moved in and out of the core at one specific location for a short time period. Such a local perturbation is intended to trigger all possible modes of oscillation. In a damped system a simulation time of 15 – 20 seconds is normally sufficient to determine DR and natural frequency. These parameters are evaluated either by a graphical interpretation of the time plots or by fitting a second order system model in the frequency domain. To determine limit-cycle amplitudes or to identify higher mode patterns, the simulation needs to be extended up to the range of 100 seconds.

Exercises have been done in order to determine whether DR would show a dependency on the perturbation used to initiate the transient calculation. Various modest ** disturbances were applied (insertion and withdrawal of control rods, pressure boundary disturbance, single symmetric and asymmetric control rod(s), etc.). The conclusion is that results are always in good agreement ($\pm 2\%$) regardless of the type of perturbation provided that its magnitude is not large enough to trigger non-linear properties, and that it also triggers the proper dynamics. How the disturbance should be performed to fulfill these requirements is stated in the code stability methodology.

The RAMONA-3 based methodology uses a neutronics time step value of 50 milliseconds (ms). The hydraulic time step is subordinate to the neutronic time step and therefore will never exceed the maximum neutronic time step. For the RAMONA-5 calculations the methodology has been revised to allow a maximum neutronic time step of 25 ms. The S3K stability calculations are performed using neutronic time steps of 50 ms and four hydraulic time steps per neutronic time step (i.e. a hydraulic time step of 12.5 ms). However, the POLCA-T calculations are performed using equal time steps for both neutronics and hydraulics of 10 ms.

The PR3 and SR5 calculations are limited to the less stable recordings 4, 6, 8 and 10.

5.5 Results of Stability Calculations

The results from the different organizations are compared in terms of the stability parameters decay ratio and resonance frequency against the measurements evaluated by PSI in Tables IV and V.

Table IV: Summary of measured and calculated results in cycle 19

Case	DECAY RATIO							RESONANCE FREQUENCY						
	Measured	Predicted by Code						Measured	Predicted by Code					
	PSI	PR3	AR3	SR5	WR5	S3K	P-T	PSI	PR3	AR3	SR5	WR5	S3K	P-T
1	0.43±0.07		0.44		0.43	0.45	0.35	0.68±0.02		0.64		0.60	0.64	0.62
3	0.46±0.07		0.54		0.53	0.53	0.45	0.67±0.02		0.66		0.60	0.64	0.65
4	0.55±0.06	0.58	0.53	0.58	0.55	0.57	0.48	0.70±0.01	0.68	0.67	0.60	0.63	0.66	0.71
5	0.49±0.07		0.51		0.48	0.54	0.45	0.65±0.02		0.65		0.59	0.64	0.67
6	0.68±0.09	0.74	0.69	0.67	0.66	0.71	0.65	0.66±0.02	0.67	0.64	0.59	0.59	0.61	0.69
7	0.59±0.06		0.52		0.50	0.59	0.54	0.63±0.02		0.62		0.56	0.61	0.65
8	0.71±0.04	0.72	0.69	0.67	0.64	0.73	0.73	0.63±0.01	0.65	0.61	0.57	0.55	0.59	0.67
9	0.40±0.11		0.41		0.40	0.30	0.37	0.47±0.02		0.48		0.40	0.44	0.45
10	0.64±0.05	0.64	0.58	0.64	0.57	0.57	0.61	0.59±0.01	0.61	0.58	0.52	0.48	0.56	0.59
11	0.54±0.10		0.57		0.53	0.48	0.52	0.54±0.02		0.54		0.45	0.52	0.53

For statistical evaluation of the results the mean deviation (bias):

$$\Delta DR_{mean} = \frac{1}{n} \sum_{i=1}^n (DR_{calc_i} - DR_{meas_i}) \quad (1)$$

** For instance for POLCA-T disturbances of up to 3% of total core power were applied

and the standard deviation are used:

$$\sigma_{\Delta DR} = \sqrt{\frac{1}{n-1} \sum_{i=1}^n ((DR_{calc_i} - DR_{meas_i}) - \Delta DR_{mean})^2} \quad (2)$$

Table V: Summary of results deviations in cycle 19

Case	DECAY RATIO						RESONANCE FREQUENCY					
	Calculated - Measured						Calculated - Measured					
	PR3	AR3	SR5	WR5	S3K	P-T	PR3	AR3	SR5	WR5	S3K	P-T
1		0.01		0.00	0.02	-0.09		-0.04		-0.08	-0.04	-0.07
3		0.08		0.07	0.07	-0.01		-0.01		-0.07	-0.03	-0.02
4	0.03	-0.02	0.03	0.00	0.02	-0.07	-0.02	-0.03	-0.10	-0.08	-0.04	0.01
5		0.02		-0.01	0.05	-0.04		0.00		-0.06	-0.01	0.02
6	0.06	0.01	-0.01	-0.02	0.03	-0.03	0.01	-0.02	-0.07	-0.07	-0.05	0.03
7		-0.07		-0.09	0.00	-0.05		-0.01		-0.07	-0.02	0.02
8	0.01	-0.02	-0.04	-0.07	0.02	0.02	0.02	-0.02	-0.06	-0.08	-0.04	0.04
9		0.01		0.00	-0.10	-0.03		0.01		-0.07	-0.03	-0.02
10	0.00	-0.06	0.00	-0.07	-0.07	-0.03	0.02	-0.01	-0.07	-0.11	-0.03	0.00
11		0.03		-0.01	-0.06	-0.02		0.00		-0.09	-0.02	-0.01
Bias	0.025	-0.001	-0.005	-0.020	-0.002	-0.034	0.008	-0.013	-0.075	-0.077	-0.031	0.002
Std. dev.	0.026	0.044	0.029	0.047	0.056	0.030	0.019	0.015	0.017	0.013	0.012	0.031

5.5.1 Decay ratio

Comparison of calculated decay ratios to the official measured values is shown in Figure 5. The diagonal line illustrates perfect match between measured and calculated values and the two parallel lines on either sides represent 1σ of the measurement uncertainty (± 0.1) deviation in decay ratio.

On a qualitative basis it can be concluded from Table IV that for all measurement points global damped oscillations are predicted by each combination of input modelling / transient code. Furthermore, it can be concluded from Fig. 5 on a quantitative basis that all results of decay ratio show reasonable agreement with the measured values.

From Table IV it can be noticed that both S3K and AR3 show remarkable small mean deviations. S3K is slightly more conservative than AR3 for high decay ratios ($DR \geq 0.55$) whereas AR3 deviates a slightly not conservative trend at high DR values. SR5 shows also an excellent agreement with the measured values but its analysis (same as PR3's analysis) is solely limited to the four (out of five) recordings that showed less stability (4, 6, 8 and 10, 7 not included) with measured $DR \geq 0.55$. PR3 and WR5 show moderate biases being PR3 always conservative. WR5 shows an almost perfect agreement with measured values for low decay ratios ($DR \leq 0.55$) but rather large not conservative trend for high decay ratios.

Similarly it can be observed in Table V that the results from PR3, SR5 and P-T show the smaller standard deviations. While PR3 and SR5 have limited analysis, P-T shows consistently non conservative biases for the 10 analyzed recordings. This behavior is not yet explained but it can not dispute the predictable capacities of the code.

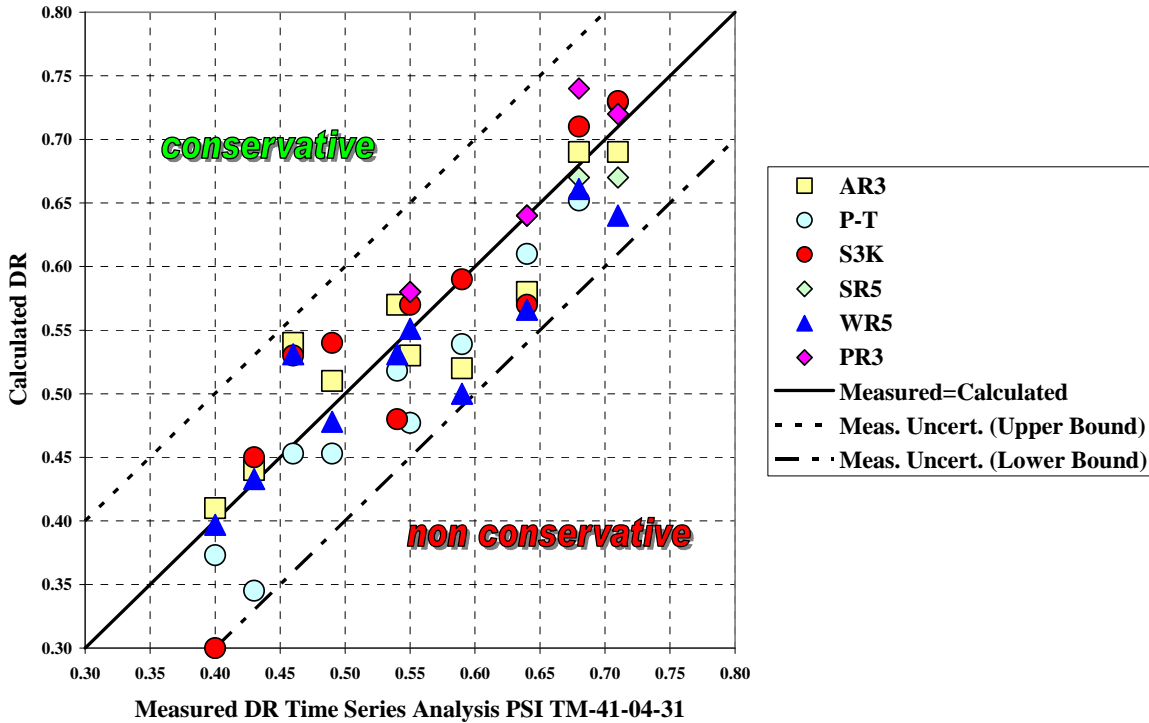


Figure 5: Code Performance with regards to the Decay Ratio

All combinations of input modeling / transient codes that have analyzed the totality of the recordings (S3K, P-T, WR5) show that recording 4 is less stable than recording 3 (see Fig. 3). This is correct since the removal of shallow rods providing for a more bottom peaked axial power distribution in recording 4 degraded the core stability.

Although limited to the aforementioned less stable four recordings a comparison between the RAMONA 5 calculations (SR5 and WR5) is interesting. SR5 shows better agreement and is more conservative. As WR5 have been setup using the 1½-group neutronics their results should be somewhat comparable to the ones coming from the RAMONA-3 calculations (PR3, AR3). This is fully confirmed. While the PR3 results are very conservative, the AR3 results seem normally to be slightly more conservative than the results from WR5. However a trend between those results is evident.

The comparison between the advanced codes S3K and P-T is more challenging. Except for the recording 8 (largest DR = 0.71) where both codes perfectly agree S3K shows a more conservative behaviour. A clear trend can not be defined.

Besides, all codes except PR3 assessed correctly that the less damped case corresponds to recording 8.

The benchmark could not confirm a general relation between the steady state power profile prediction and the calculated DR. Good agreement of the axial power shape indicates that the model is sound, but this necessary condition is not sufficient to always guaranty a good match to the measured DR.

Finally, the benchmark could neither confirm a clear dependence of DR on the spatial and time discretization. This is not because the numerical methods do not interfere with the physical properties, but

because time step and nodalisation have been chosen in a magnitude that this impact becomes insignificant (small enough time-step and space discretization adapted to velocity of fluid). The choice of time step and space discretization is controlled by the code methodology and the validation.

5.5.2 Resonance frequency

The comparison of the code dependant frequencies to the official measured values is shown in Figure 6. The diagonal line illustrates perfect match between measured and calculated values and the two parallel lines on either sides represent $2\sigma = 0.04$ deviation in oscillation frequency.

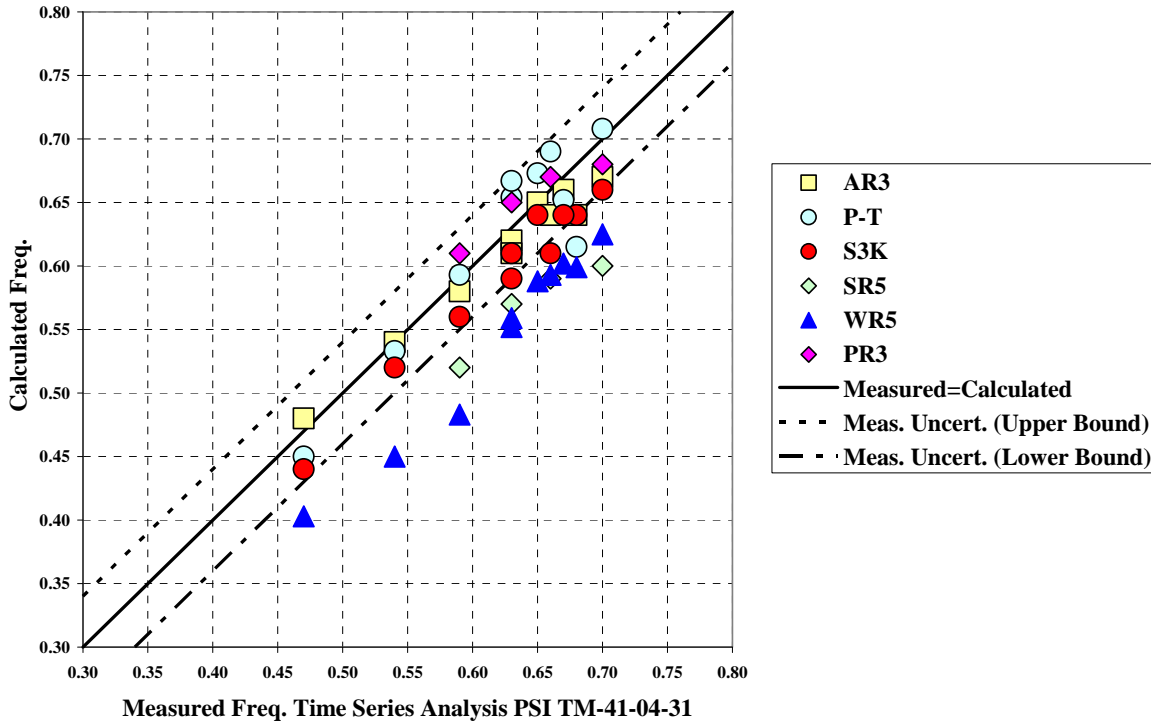


Figure 6: Code Performance with regards to the Resonance Frequency

It can be observed in Fig. 6 and Table IV that S3K, SR5 and WR5 systematically underestimate the measured values. S3K shows smaller deviations than the RAMONA calculations but a trend is evident. Interesting is that similar trend can be observed also by AR3, but the bias seems to have been removed causing over prediction at low flow (recording 9) and under predicting at high flows (recordings 1, 3 and 4). PR3 tends also to over predict the frequency values (except for recording 4). Finally P-T takes all the credits in this topic. No trend is noticeable. It manages a perfect agreement for recording 10, the one located at the centre of the exclusion region.

6. CONCLUSIONS

All methods and codes investigated in this work provide flexible and accurate tools for BWR stability analysis. The qualification results of decay ratio against the KKL cycle 19 stability data have fulfilled the expectations. All results show good agreement with the measured values within the bounds of the measurement uncertainty.

In the study it has been demonstrated that the advanced methods (S3K, P-T, R5) are not necessarily making it better than for instance AR3 for a complex core loading like the KKL cycle 19 core with a substantial amount of last generation fuel assemblies. The post-analysis of the stability data has shown that the expertise of the organizations dealing with old codes can still close the gap opened after the arrival of modern codes relying more on their advanced physical modeling. However the fact that P-T and S3K are doing so well using more in depth in the true physics and denying the traditional “engineering assumptions” often used in stability analysis, distinguish these codes primary for predictive calculations.

The analysis has also demonstrated that some work is still to be done in some codes to reduce the biases predicting the resonance frequency. This can be tricky since it can be related to the accuracy of the void correlation at the operating conditions where stability is an issue. As a rule void correlations are adjusted for operation at full power. In any case the continue development of the thermal-hydraulics can solve this problem in a relatively short term.

The performance of the steady state simulators against the TIP measurements shows that POLCA 7 and PRESTO-2 over predict the power bottom peak. In combination with R3, that usually also provides larger peaking factors than the steady state simulators this effect can lead to un-physical reduction of the stability margins.

Finally we need to remark that all the conclusions promulgated in this work are based on the reliability of the evaluation of the measurement data by PSI. The GSE evaluation gives larger DR for almost all the measured points. Comparing the code performances to those results would result in a much more non conservative behavior of all the codes leading to a different conclusion.

ACKNOWLEDGMENTS

The first author would primarily like to acknowledge the organizations that have made possible the conclusion of this work with special emphasis for the involved persons, the co-authors and hidden helpers, who have struggled during these years with the input modeling and the sometimes ungrateful codes. Additionally one should not forget to thank the intellectual help received from three personalities of the European BWR stability society, all of them professors in distinguished Universities, who have made a deep impression on the first author and have contributed to the better understanding of the stability problem in BWR: Dieter Hennig, Germany, Tim van der Hagen, The Netherlands and José Luis Muñoz Cobos, Spain.

REFERENCES

1. C. Aguirre, “KKL C19 Core Stability Test after Power Uprate”, KKL Technischer Bericht BET/02/128, 4.10.2003
2. A. Schmidt et al., “Stability Behavior of ATRIUM 10XM Reload Assemblies for KKL”, Work Report A1C-1333390-1, 4.29.2008
3. H. Ferroukhi et al, “KKL BOC19 Stability Measurements - Time Series Analysis and RAMONA-3 calculations”, PSI TM-41-03-02, 3.31.2003
4. G. Grandi, “KKL Stability Test Analysis with Ramona 5”, SSP Memorandum, 11.29.2005
5. L. Belblidia et al, “SIMULATE 3K stability benchmarking and predictive calculations of Leibstadt”, *Proceeding International. Conference. Nuclear Power a Sustainable Resource (PHYSOR 2008)*, Interlaken, Switzerland, September 14-19 (2008)
6. C. Jönsson, C., “KKL SVEA 96 Optima 3 Stability calculations”, WSE Report SET 08-140, Rev. 1, 11.13.2008
7. M. Thunman, “POLCA T Validation at Kernkraftwerk Leibstadt Stability measurements”, WSE Report SES 05-167, Rev. 1
8. A. Dokhane et al., “A Reactor Noise Analysis Methodology for BWR Core Stability Evaluation: Application and Assessment to Leibstadt Stability Tests”, *Proceeding American Nuclear Society Topical Meeting in Mathematics and Computation*, Avignon, France, September 12-15, 2005
9. R Oguma et al, “Stability Investigation Based on Noise Analysis for Cycle 10, 13, and 19 Operations at BWR Kernkraftwerk Leibstadt”, Report GSE-04-005, 4.16.2004
10. R. T. Lahey, Jr. F. J. Moody, *The Thermal-Hydraulics of a Bowling Water Nuclear Reactor*, American Nuclear Society, Illinois, USA (1977)
11. J. March-Leuba, J. M. Rey, “Coupled thermohydraulic-neutronic instabilities in boiling water nuclear reactors: a review of the state of the art”, *Nuclear Engineering and Design*, **Vol. 145**, pp. 99 (1993)
12. D. Hennig, “A Study on Boiling Water Reactor Stability Behavior”, *Nuclear Technology*, **Vol. 126**, pp. 10-30 (1999)
13. C. Aguirre et al, “Natural Circulation and Stability performance of BWRs (NACUSP)”, *Nuclear Engineering and Design*, **Vol. 235**, pp. 401-409 (2005)
14. B. Askari et al, “Some Remarks on Time Series Analysis for BWR Stability Studies”, *Proceeding American Nuclear Society Topical Meeting International Conference on Mathematical Methods to Nuclear Applications*, Salt Lake City, USA, September 9-13 (2001)